Fig. 2. He–Ne laser light propagating in Si_3N_4 waveguide.
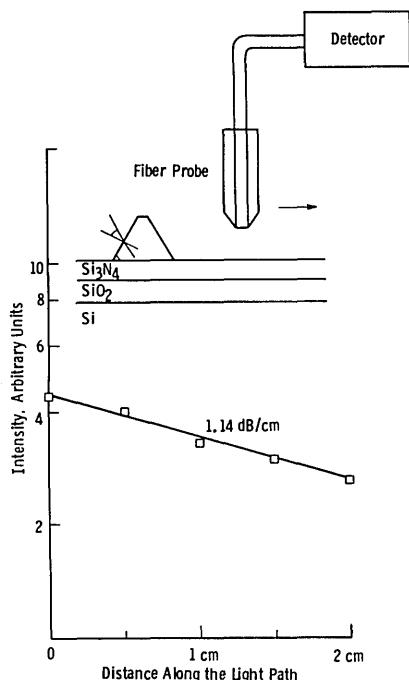

Fig. 3. Waveguide loss measurement.

We have demonstrated that reasonably high optical waveguide performance can be obtained in plasma-deposited Si_3N_4 films. We expect that lower propagation loss factors can be obtained with careful optimization of the films for this application and that other plasma-deposited inorganic films can be used as low-loss waveguides.

References

1. J. R. Hollahan and R. S. Rosler, "Plasma Deposition of Inorganic thin films," in *Thin Film Processes*, J. L. Vossen and W. Kern, Eds. (Academic, New York, 1978).
2. E. P. G. T. van de Ven, Solid State Technol. 24, No. 4, 167 (1981).
3. W. Stutius and W. Streifer, Appl. Opt. 16, 3218 (1977).
4. P. K. Tien, Appl. Opt. 10, 2395 (1971).

Photorefractive incoherent-to-coherent optical converter

Y. Shi, D. Psaltis, A. Marrakchi, and A. R. Tanguay, Jr.

Y. Shi and D. Psaltis are with California Institute of Technology, Division of Engineering & Applied Science, Pasadena, California 91125; the other authors are with University of Southern California, Departments of Electrical Engineering and Materials Science, Optical Materials & Devices Laboratory, Los Angeles, California 90089.

Photorefractive materials have been extensively used in recent years as real-time recording media for optical holography.[1,2] One prospective application of real-time holography is in the area of optical information processing; for example, the correlation between two mutually incoherent images has recently been demonstrated in real time in a four-wave mixing geometry.[3] Often, however, the information to be processed exists only in incoherent form. High performance spatial light modulators[4] are thus necessary in many optical information processing systems to convert incoherent images to coherent replicas for subsequent processing. We report in this Communication the successful demonstration of real-time incoherent-to-coherent images transduction through the use of holographic recording in photorefractive crystals. Several possible configurations and experimental results are presented.

The interference of two coherent beams in the volume of a photorefractive crystal generates nonuniformly distributed free carriers, which are redistributed spatially by diffusion and/or drift in an external applied field. The subsequent trapping of the free carriers in relatively immobile trapping sites results in a stored space-charge field, which in turn modulates the index of refraction through the linear electrooptic effect.[5] Thus a volume phase hologram is recorded. If the two coherent beams are plane waves, a uniform phase grating is established. An incoherent image focused in the volume of the photorefractive material will spatially modulate the charge distribution stored in the crystal. This spatial modulation can be transferred onto a coherent beam by reconstructing the holographic grating. The spatial modulation of the coherent reconstructed beam will then be a negative replica of the input incoherent image. The holographic
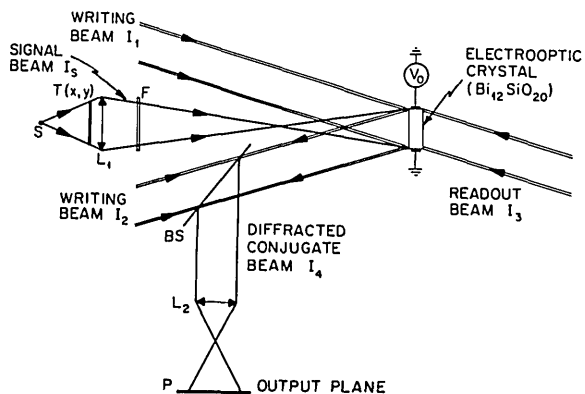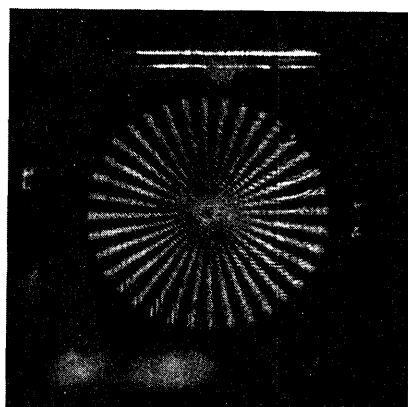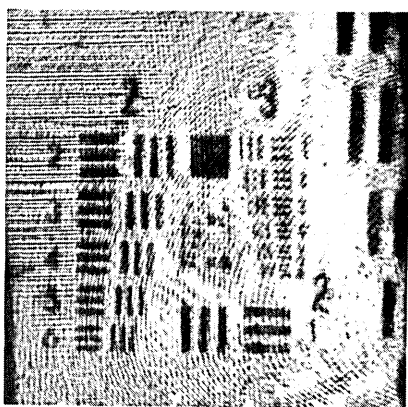
Fig. 1. Experimental setup for incoherent-to-coherent conversion with phase conjugation in four-wave mixing. The writing beams I_1 and I_2 and the reading beam I_3 are generated from an argon laser (λ = 514 nm). The phase conjugate beam I_4 is diffracted at the same wavelength. The transparency $T(x,y)$ is illuminated with a xenon arc lamp S and imaged on the BSO crystal with the optical system L_1 through a filter F (λ = 545 nm). BS is a beam splitter, and P is a polarizer placed in the output plane.

(a)

(b)

Fig. 2. Incoherent-to-coherent conversion utilizing phase conjugation in four-wave mixing: (a) spoke target; (b) USAF resolution target. The group 3.6, corresponding to a resolution of 14.3 lp/mm, is well resolved.

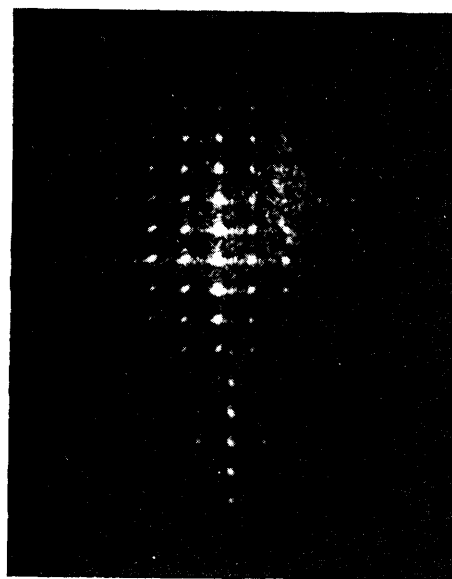Fig. 3. Photorefractive incoherent-to-coherent conversion of a transparency with grey levels.

Fig. 4. Fourier transform of a grid pattern formed after a photorefractive incoherent-to-coherent conversion of the grid pattern pattern image.

grating can be recorded before, during, or after the crystal is exposed to the incoherent image. Therefore, a number of operating modes are possible. These include the grating erasure mode (GEM), the preerasure writing mode (PEWM), and the simultaneous erasure writing mode (SEWM), among others.

In the grating erasure mode, a uniform grating is recorded by interfering the two writing beams in the photorefractive crystal. This grating is then selectively erased by incoherent illumination of the crystal is then selectively erased by incoherent illumination of the crystal with an image-bearing beam. The incoherent image may be incident either on the same face of the crystal as the writing beams or on the opposite face. When the absorption coefficients of the writing and image-bearing beams give rise to significant depth nonuniformity within the crystal, these two cases will have distinct wavelength-matching conditions for response optimization.

In the preerasure writing mode, the crystal is preilluminated with the incoherent image-bearing beam prior to grating formation. This serves to selectively decay (enhance) the applied transverse electric field in exposed (unexposed) regions of the crystal. After this preexposure, the writing beams are then allowed to interfere within the crystal, causing grating

formation with spatially varying efficiency due to vast differences in the local effective applied field. This technique will also work in the diffusion limit with no external applied field by means of a similar physical mechanism.

In the simultaneous erasure writing mode, the conventional degenerate four-wave mixing geometry is modified to include simultaneous exposure by an incoherent image-bearing beam, as shown schematically in Fig. 1. Diffraction by a phase grating in the four-wave mixing configuration has been modeled following two different approaches.[6,7] Common to both analyses, the diffracted intensity is proportional to both the readout intensity and the square of an effective modulation ratio, in the first-order approximation, and assuming no pump depletion. In addition, a uniform beam incident on the photosensitive medium at an arbitrary angle decreases the modulation ratio and hence the overall diffraction efficiency.[8] In the SEWM configuration, these effects can be combined with the diffraction of a conjugate beam in a four-wave mixing geometry to perform the incoherent-to-coherent image conversion. In particular, this conversion can be regarded as caused by selective spatial modulation of the grating by spatial encoding of the incoherent erasure beam. It should be noted here that a related image encoding process could be implemented in a nonholographic manner by premultiplication of the image with a grating.[9]

In our experiments, we have successfully produced incoherent-to-coherent conversions in all three operating mode configurations as well as in several modifications of the basic arrangements described above. We present here experimental results from our implementations of the simultaneous erasure writing mode.

The experimental arrangement in one implementation is as shown in Fig. 1. The two plane wave writing beams (labeled I_1 and I_2) are generated from an argon laser ($\lambda = 514$ nm) and interfere inside the photorefractive crystal to create a phase volume hologram. The readout beam I_3, collinear with I_1 to satisfy the Bragg condition, diffracts the phase conjugate beam I_4 at the same wavelength and with increased diffraction efficiency when a transverse electric field is applied to the electrooptic medium. An incoherently illuminated transparency $T(x,y)$ with intensity $I_s(x,y)$ (either quasi-monochromatic or white light) is imaged in the plane of the crystal. The beam splitter BS separates the diffracted signal from the writing beam; the Polaroid filter P in the output plane eliminates the unwanted scattered light to enhance the signal-to-noise ratio.[10] The photorefractive material utilized was a single crystal of bismuth silicon oxide (BSO), cut to expose polished (110) faces, and of dimensions $7.3 \times 6.9 \times 1.3$ mm^3.

A transverse electric field $E_0 = 4$ kV/cm was applied along the $[\bar{1}10]$ axis perpendicular to the polished faces. The carrier frequency of the holographic grating, $f = 300$ lp/mm, was within the optimum range for the drift-aided charge transport process.[11] The vertically polarized coherent writing beam and signal intensities were $I_{1,2} = 0.4$ mW/cm^2 and $I_s = 8$ mW/cm^2, respectively. Figure 2 shows the converted images obtained from two binary transparencies (a spoke target and a USAF resolution target). The illumination was provided by a xenon arc lamp through a broadband filter centered at $\lambda = 545$ nm (FWHM = 100 nm). An approximate resolution of 15 lp/mm was achieved without optimizing factors such as the optical properties and quality of the crystal, the depth of focus in the bulk of the medium, the carrier frequency of the grating, and the relative intensities and wavelengths of the various beams. This spatial bandwidth is comparable with that obtained with a PROM[12] or a liquid crystal light valve.[13]

The image shown in Fig. 3 demonstrates the capability of the technique to reproduce many grey levels. To obtain this image, a negative transparency was illuminated with blue light ($\lambda = 488$ nm) derived from an argon laser and was focused on the BSO crystal. The holographic grating was recorded with green light ($\lambda = 514$ nm) and read out with an auxiliary red beam ($\lambda = 6328$ Å).

The 2-D Fourier transform formed by a lens after the incoherent-to-coherent conversion of a grid pattern is shown in Fig. 4. The fundamental spatial frequency of the grid was ~1 lp/mm. The existence of several diffracted orders and the well-focused diffraction pattern are positive indications that the device is suitable for coherent optical processing operations.

Although these results are preliminary, they clearly demonstrate the feasibility of real-time incoherent-to-coherent conversion utilizing phase conjugation in photorefractive BSO crystals. This device has potential for incoherent-to-coherent conversion with high resolution, which can be realized by optimizing the optical properties and quality of the crystal, the depth of focus in the bulk of the medium, the carrier frequency of the grating, and the relative intensities and wavelengths of the various beams. In addition, such a device is quite attractive from considerations of low cost, ease of fabrication, and broad availability. With such a device, numerous optical processing functions can be directly implemented that utilize the flexibility afforded by the simultaneous availability of incoherent-to-coherent conversion and volume holographic storage.

References

1. P. Gunter, "Holography, coherent light amplification, and optical phase conjugation," Phys. Rep. in press (1983).
2. D. M. Pepper, Opt. Eng. 21, 156 (1982).
3. J. O. White and A. Yariv, Appl. Phys. Lett. 37, 5 (1980).
4. A. R. Tanguay, Jr., in *Proceedings, ARO Workshop on Future Directions for Optical Information Processing, Lubbock, Tex., May, 1980* (1981), pp. 52–77.
5. D. L. Staebler and J. J. Amodei, J. Appl. Phys. 43, 1042 (1972).
6. J. Feinberg, D. Heiman, A. R. Tanguay Jr., and R. W. Hellwarth, J. Appl. Phys. 51, 1297 (1980).
7. N. V. Kakhtarev, V. B. Markov, S. G. Odulov, M. S. Soskin, and V. L. Vinetskii, Ferroelectrics 22, 961 (1979).
8. W. D. Cornish and L. Young, J. Appl. Phys. 46, 1252 (1975).
9. R. Grousson and S. Mallick, Appl. Opt. 19, 1762 (1980).
10. J. P. Herriau, J. P. Huignard, and P. Aubourg, Appl. Opt. 17, 1851 (1978).
11. J. P. Huignard, J. P. Herriau, G. Rivet, and P. Gunter, Opt. Lett. 5, 102 (1980).
12. Y. Owechko and A. R. Tanguay, Jr., Opt. Lett. 7, 587 (1982).
13. P. Aubourg, J. P. Huignard, M. Hareng, and R. A. Mullen, Appl. Opt. 21, 3706 (1982).